Structural Characterization of Na,K-ATPase from Shark Rectal Glands by Extensive Trypsinization†

Mikael Esmann,*,‡ Ashish Arora,§,|| Arvid B. Maunsbach,⊥ and Derek Marsh§

Department of Biophysics, Institute of Physiology and Biophysics, University of Aarhus, DK-8000 Aarhus C, Denmark, Max-Planck-Institut für biophysikalische Chemie, Abteilung Spektroskopie, 37077 Göttingen, Germany, and The Water and Salt Research Centre, Department of Cell Biology, Institute of Anatomy, University of Aarhus, DK-8000 Aarhus C, Denmark

Received August 9, 2005; Revised Manuscript Received November 15, 2005

ABSTRACT: Extensive trypsinization of Na,K-ATPase from the salt gland of *Squalus acanthias* removes about half of the extramembranous protein mass of the α-subunit, while leaving the *β*-subunit intact. Sequence analysis and epitope recognition of the remaining α-peptides show that transmembrane segments M1/M2 and M3/M4 are present when trypsinization is performed in either NaCl or RbCl. The M5/M6 segment and the intact 19-kDa peptide (M7-M10) are detected in Rb-trypsinized membranes but not in Na-trypsinized membranes. The L7/L8 loop is associated with Na-trypsinized membranes, indicating the presence of an M7/M8 or M8/M9 fragment. Freeze-fracture electron microscopy of both Rb- and Na-trypsinized membranes reveals intramembranous particles that indicate a retained cluster of peptides, even in the absence of an intact 19-kDa fragment. The rotational diffusion of covalently spin-labeled trypsinized complexes is studied in the presence of poly(ethylene glycol) or glycerol by using saturation transfer electron spin resonance. Rotational correlation times in aqueous poly(ethylene glycol) are longer than in glycerol solutions of the same viscosity and increase nonlinearly with the viscosity of the suspending medium, indicating that poly(ethylene glycol) induces aggregation of the tryptic peptides (and *β*-subunit) within the membrane. The aggregates of enzyme trypsinized in the presence of NaCl are larger than those for enzyme trypsinized in RbCl, at both low and high aqueous viscosities. Similarities in mobility for native and Rb-trypsinized enzymes suggest either a change in average orientation of the spin-label upon trypsinization or that trypsinization leads to a reorganized protein structure that is more prone to aggregation.

The Na,K-ATPase (E.C. 3.6.3.9) couples hydrolysis of intracellular ATP to vectorial transport of Na^+ and K^+ against their electrochemical gradients. The enzymatic cycle consists of a number of conformational changes involving nucleotide binding, cation occlusion, and phosphorylation/dephosphorylation of the protein (reviewed by Møller et al. (*1*) and Kaplan (*2*)). The enzyme is composed of two subunits of molecular masses 113 kDa (the α-subunit)[1] and 35 kDa (the *β*-subunit). The α-subunit traverses the membrane 10 times and bears a large and a smaller cytoplasmic loop. The *β*-subunit has one transmembrane stretch, and most of the protein mass resides in the extracellular space, together with about 10 kDa of carbohydrate at three glycosylation sites. The α-subunit bears the nucleotide and phosphorylation sites, and chemical modification, as well as mutagenesis, studies suggest that the cation-binding sites are located within the transmembrane domains of the α-subunit. At present, the three-dimensional structure of Na,K-ATPase is known at about 9 Å resolution (*3*, *4*). The Ca-ATPase, which has a 30% identity and 65% homology to Na,K-ATPase, has been crystallized in several conformations revealing the detailed protein structure at the 3 Å level (*5*−*7*). Here, the Ca-ATPase structure in the Ca-bound form (*5*) is used as a model for the protein structure of the Na,K-ATPase α-subunit (see Figure 1 for an outline).

† Financial support was received from the Human Frontier Science Program (RG 511/M to M.E.) and the Danish Medical Research Council (Grant Nos. 52-00-0914 to M.E. and 22-02-0352 to A.B.M.).

* Corresponding author: Mikael Esmann, Department of Biophysics, Institute of Physiology and Biophysics, Ole Worms Alle 185, DK-8000 Aarhus C, Denmark. Phone: (45) 89 42 29 30. Fax: (45) 86 12 95 99. E-mail: me@biophys.au.dk.

‡ Department of Biophysics, Institute of Physiology and Biophysics, University of Aarhus.

§ Max-Planck-Institut für biophysikalische Chemie.

|| Current address: Molecular and Structural Biology, Central Drug Research Institute, Lucknow 226 001, India.

⊥ The Water and Salt Research Centre, Department of Cell Biology, Institute of Anatomy, University of Aarhus.

[1] Abbreviations: α-subunit, the 113 kDa catalytic subunit; *β*-subunit, the 35 kDa glycosylated subunit; CAPS, 3-(cyclohexyl)propanesulfonic acid; CDTA, *trans*-1,2-cyclohexylenedinitrilotetraacetic acid; Class I, the sulphydryl groups reactive in the presence of 25% glycerol; Class II, the sulphydryl groups labeled with thiol reagents during inactivation of overall Na,K-ATPase activity; ESR, electron spin resonance spectroscopy; IMP, intramembrane particle; M1/M2, the tryptic fragment with N-terminal D^{75}; M3/M4, the tryptic fragment with N-terminal I^{270}; M5/M6, the tryptic fragment with N-terminal Q^{744}; M7-M10, the tryptic fragment with N-terminal T^{841}; L7/L8, the extracellular loop containing epitope 896−910; Na-T, membranes trypsinized in the presence of Na^+; NEM, *N*-ethylmaleimide; PEG, poly(ethylene glycol); PVDF, polyvinylidine difluoride; Rb-T, membranes trypsinized in the presence of Rb^+; SDS, sodium dodecyl sulfate; SERCA, Ca-ATPase predominant in sarcoplasmic reticulum; STESR, saturation transfer ESR; Tris, tris(hydroxymethyl)aminomethane; 5-MeClHgMSL, *trans*-3-methoxycarbonyl-4-(4′-chloromercuri-benzamido)methyl-1-oxyl-2,2,5,5-tetramethylpyrrolidine; 19-kDa membranes, the membranous Na,K-ATPase preparation remaining after extensive trypsinization in the presence of RbCl.

10.1021/bi051573x CCC: $33.50
Published on Web 12/22/2005

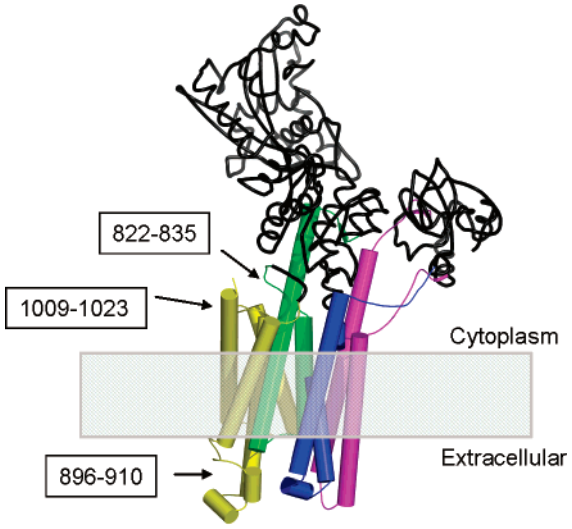

FIGURE 1: Outline of the assumed topography of the Na,K-ATPase α-subunit using the Ca-ATPase crystal structure as template (*5*). The peptides corresponding to the tryptic fragments residing in the membranes are shown in magenta (M1/M2, SERCA residues 36−137), blue (M3/M4, SERCA residues 235−313), green (M5/M6, SERCA residues 731−819), and yellow (M7-M10, SERCA residues 826−994) with helical structures as cylinders. The parts of the α-subunit removed by trypsin are given in black. The recognition site for the antibodies against 822−835 and 896−910 as well as the C-terminal 1009−1023 are indicated (numbers refer to shark Na,K-ATPase sequence), and the membrane domain is in gray. This figure was prepared using PyMOL (*49*).

Extensive proteolytic degradation of the constituent polypeptides of P-type ATPases, which in addition to Na,K-ATPase and Ca-ATPase includes the H,K-ATPase, has been used to elucidate structural properties such as transmembrane disposition, content of α-helical and β-sheet structure, and interaction between membrane-bound segments of the polypeptides. In extensive studies on Na,K-ATPase, Karlish and co-workers probed the spatial organization of the trypsinized protein, both in the membrane-bound form (*8*−*10*) and in the detergent-solubilized state (*11*). Askari and co-workers have studied the interaction of these trypsinized preparations with cations, ouabain, and ATP (*12*, *13*). Proteolysis with trypsin and proteinase K leads to membranous preparations with residual protein of predominantly α-helical structure for Ca-ATPase (*14*, *15*) or both α-helical and β-sheet structure for H,K-ATPase (*16*). The latter has also been found in trypsinized Na,K-ATPase membranes (*17*). The proteolyzed preparations, therefore, form a well-defined basis for detailed studies on the intramembranous structure of P-type ATPases by spectroscopic methods, because much of the cytoplasmic protein, which otherwise masks the contributions of the membranous domains, is absent (cf. Figure 1).

In the present work, we characterize, in some depth, Na,K-ATPase preparations from the salt gland of *Squalus acanthias* that have been trypsinized extensively in the presence of either Rb^+ (a congener for K^+) or Na^+. Sequence analysis and epitope mapping are used to identify tryptic fragments; electron microscopy is used to visualize intramembrane structure, and rotational diffusion measurements in different aqueous media are used to investigate aggregation state and extramembranous exposure of the tryptic peptides. Special attention is given to membranes trypsinized in Na^+ because, unlike the kidney enzyme (*8*), this results in further degradation of a 19-kDa fragment that is found in Rb-trypsinized preparations, with concomitant loss of Rb-occlusion capacity (*18*).

MATERIALS AND METHODS

Materials. Poly(ethylene glycol) with an average molecular weight of 4000 and molecular weight markers (MW-SDS-17S) were obtained from Sigma Chemical Co. (St. Louis, MO), and analytical grade glycerol was from Merck (Darmstadt, Germany). The chloromercuri-spin label, 5-MeClH-gMSL, was prepared as previously described (*19*).

Enzyme Preparation and Assay. Membranous Na,K-ATPase was prepared from the salt gland of *S. acanthias* according to the method of Skou and Esmann (*20*), except omitting the treatment with saponin. Enzymatic activities and protein contents were determined as previously described (*21*).

Spin-Labeling of Na,K-ATPase. The protein was spin-labeled covalently on Class II−SH groups with 5-MeClH-gMSL, after prelabeling Class I−SH groups with *N*-ethylmaleimide, as described earlier (*18*): Na,K-ATPase (approximately 1 mg/mL) was incubated at 23 °C with 0.1 mM NEM in 30 mM histidine (pH 7.0 at 23 °C), 5 mM CDTA, 150 mM KCl, and 36% (v/v) glycerol for 60 min. The reaction was stopped by addition of 2-mercaptoethanol (1 mM), and the membranes were washed by centrifugation in 20 mM histidine (pH 7.0 at 20 °C) and 25% (v/v) glycerol, at 200 000*g*. Selective spin-labeling of SH-groups that are essential for the overall Na,K-ATPase activity was performed as follows (*19*): prelabeled Na,K-ATPase (see above) was incubated for 30 min with 6 μM 5-MeClHgMSL at 23 °C in 30 mM histidine (pH 7.4 at 37 °C) in the presence of 150 mM KCl and 5 mM CDTA. The reaction was stopped by addition of 1 mM 2-mercaptoethanol. The membranes were washed by centrifugation in 20 mM histidine (pH 7.0 at 20 °C) and 25% (v/v) glycerol at 200 000*g*. The spin-labeled enzyme was stored in 20 mM histidine and 25% (v/v) glycerol at −20 °C.

Trypsinization of Na,K-ATPase. Native or spin-labeled Na,K-ATPase membranes were incubated at a concentration of 0.9 mg/mL with 10 mM RbCl or NaCl in 15 mM histidine and 1 mM CDTA (pH 7.0 at 20 °C), and with trypsin (final concentration 0.5 mg/mL), essentially as described by Karlish et al. (*8*). After 60 min at 23 °C, a 10-fold excess by weight of trypsin inhibitor was added, in the same buffer, and the sample was allowed to stand for 10 min at 23 °C. The membranes were washed by centrifugation three times at 10 °C in a buffer containing 10 mM RbCl or NaCl, 15 mM histidine, 1 mM CDTA (pH 7.0 at 20 °C), and 25% glycerol (*18*). Samples were stored at −20 °C in this buffer. Enzyme treated as above, but omitting trypsin, serves as "control". The trypsinized samples of native enzyme were used for electron microscopy, as well as for sequence and epitope determination (see below). The spin-labeled trypsinized samples were used for ESR spectroscopy (see below).

Polyacrylamide Gel Electrophoresis. SDS−polyacrylamide gel electrophoresis was performed according to the method of Schagger and von Jagow (*22*) using 1-mm 12 or 16% gels. Membranes were dissolved in sample buffer, which contained 100 mM Na-phosphate (pH 7.7), 1% 2-mercaptoethanol, 2% SDS, and 36% urea. Samples were

heated to 100 °C for 5 min before electrophoresis. Staining was carried out using a solution of 0.25% Coomassie Blue R250/40% ethanol/10% acetic acid for 1 h, and destaining was performed in 30% ethanol/10% acetic acid. Electroblotting was carried out as described by Matsudaira (*23*), using a LKB 2051 Midget Multiblot apparatus with Problott PVDF membranes (Applied Biosystems). Only HPLC-grade solvents and Millipore-filtered or twice-distilled water were used. The electroblotting buffer contained 0.005% SDS (*23*).

Sequence Analysis of N-Terminal Peptides. After transfer to PVDF membranes, peptides separated by electrophoresis in 16% gels were stained with Coomassie Blue. The Edman degradations were carried out on a 477A instrument from Applied Biosystems with on-line analysis of the phenylthiohydantoin amino acids by reverse-phase HPLC on a 120A liquid chromatograph. The stained, electroblotted samples were cut in small pieces and placed in the cross-flow chamber. The residue numbering follows that of the α-subunit sequence (GenBank accession number AJ781093).

Epitope Identification with Antibodies. Antibodies against epitopes 822−835 (pig kidney residues 815−828), 896−910 (kidney residues 889−903), and 1009−1023 (kidney residues 1004−1018) of the α-subunit were prepared as previously described (*24*). Western blots of tryptic fragments on 16% SDS-gels were used to detect epitopes remaining associated with the membranes after extensive trypsinization. For immunocharacterization of the peptides separated by electrophoresis, these peptides were transferred—without staining—to PVDF membranes by semidry blotting (*25*). A 10 mM CAPS buffer at pH 11, containing 10% methanol, was used for the transfer. The PVDF membranes were then blocked with 0.5% Tween 20 in Na-phosphate buffer. The membranes were incubated with the primary antibodies for 1 h at 37 °C and subsequently washed with Tween 20. The primary antibodies were detected with a horseradish peroxidase-coupled goat anti-rabbit secondary antibody and visualized by staining with aminoethylcarbazole.

Electron Microscopy. The following experiment was done four times. Membrane samples from each of the three experimental conditions for trypsinization (control, prepared with 10 mM Rb^+ in the absence of trypsin; Rb-T, trypsinized in 10 mM Rb^+; Na-T, trypsinized in 10 mM Na^+) were coded and freeze-fractured. The samples were first incubated in 30% glycerol, and then were frozen in liquid nitrogen, fractured in a Balzers freeze-fracture apparatus (BAF 300, Balzers AG) at −100 °C, and shadowed unidirectionally with platinum. The replicas were examined with a Zeiss 912 Omega or a Philips 208 electron microscope. The same membrane preparations were also negatively stained with 1% uranyl acetate. The freeze-fracture micrographs were evaluated and grouped based on the distribution of intramembrane particles and their degree of clustering, before the code was broken.

ESR Spectroscopy. Spin-labeled and trypsinized membranes were pelleted in 30 mM histidine, RbCl, or NaCl, and 1 mM CDTA, pH 7.6 (at 20 °C), and gently homogenized—using a capillary pipet and an Eppendorf tube—in a small volume of the same buffer. For control enzyme (Cont.) and enzyme trypsinized in RbCl (Rb-T), the homogenization was in 100 mM RbCl, whereas the enzyme trypsinized in NaCl (Na-T) was homogenized in 100 mM NaCl. Glycerol or PEG, as concentrated solutions in the same buffer, was mixed thoroughly with the membrane suspension and taken up into a 1-mm diameter glass capillary to produce a sample of length 5 mm (*26*). Conventional (V_1-display) and saturation transfer (V_2'-display) ESR spectra were recorded as described earlier (*27*) on a Varian Century-Line 9-GHz spectrometer. Standardized sample geometry and spectrometer settings and calibrations were employed (*26*, *28*). Calibrations of the high-field diagnostic STESR line height ratio (H''/H), in terms of the rotational correlation times (τ_R^{eff}) of spin-labeled haemoglobin, were taken from Marsh (*29*):

$$\tau_R^{eff} = 407/(2.17 - H''/H) - 210\ \mu s$$

Calculation of Peptide Stoichiometry. When the 10-transmembrane model for the α-subunit was used (see, e.g., Figure 2 in ref *30*), the effect of trypsinization on molecular mass of the αβ-protomer was calculated. Assuming a glycosylation of the β-subunit of about 10 kDa per molecule (*31*) gives a protomer molecular mass of 113 + 35 + 10 = 158 kDa, for the native enzyme. The residues retained in the tryptic fragments are from the molecular weights and N-terminal analysis assumed to be 75−176 (M1/M2), 270−348 (M3/M4), 744−832 (M5/M6), and 841−1023 (M7-M10). The peptide fragments released by trypsin thus contain 569 amino acids which correspond to 40% of the mass of the native αβ-protomer (assuming an average contribution of ca. 111 Da per amino acid). The molecular mass of the trypsinized αβ-protomer is then about 95 kDa. The protein mass residing on the intracellular side of the membrane is about 87 kDa in the native αβ-protomer, which is reduced to 24 kDa by trypsin. On the extracellular side, the total mass of about 45 kDa (8 kDa of α-subunit, 27 kDa of β-subunit, and 10 kDa of carbohydrate) remains unaffected by trypsin.

Data Analysis. Data analysis was performed using the ORIGIN 6.0 software (Microcal, Amherst, CA).

RESULTS

Extensive trypsinization of Na,K-ATPase from shark rectal glands leads to a preparation with a prominent 19-kDa fragment in 12% SDS-gels, when the proteolysis is carried out in the presence of K^+ or its congener Rb^+ (see Figure 2, left panel). This is similar to the original results of Karlish et al. (*8*) on Na,K-ATPase from kidney, and we had earlier identified the same proteolysis products (M1/M2, M3/M4, M5/M6, and M7-M10) in shark membranes (*18*) as those obtained with the kidney preparation. In contrast to the behavior of the kidney preparation, we found that trypsinization of the shark membranes in the presence of NaCl leads to degradation of the 19-kDa fragment; that is, peptide bonds within the C-terminal 183 amino acids become accessible to trypsin in the E_1-form of the shark enzyme (see Figure 2, left panel). To characterize the trypsinized preparations in more detail, we have examined the overall structure with electron microscopy and also have identified N-terminal residues and antibody epitopes in the tryptic fragments.

Structure of Trypsinized Membranes As Observed by Electron Microscopy. The 12 samples from four separate experiments (each with a control, a Rb-trypsinized, and a Na-trypsinized preparation) were classified on the basis of the distribution of intramembrane particles (IMPs) in freeze-fracture. Four samples were characterized by a low degree

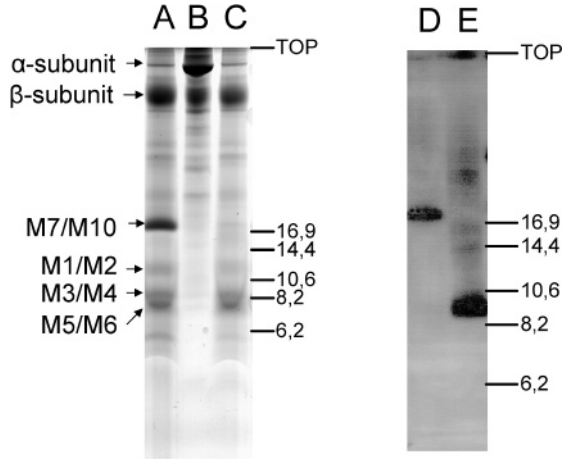

FIGURE 2: Polyacrylamide gel electrophoresis of membranous preparations of Na,K-ATPase from shark rectal glands. The left panel shows peptides separated on a 12% gel and visualized with Coomassie Blue stain. Lane A, enzyme trypsinized in RbCl; lane B, control enzyme (no trypsin); lane C, enzyme trypsinized in NaCl. The approximate positions of the 19 kDa fragment (M7-M10) as well as the tryptic peptides containing membrane spanning sequences M1/M2, M3/M4, and M5/M6 are marked. The right panel is an immunoblot of peptides separated in a 16% gel using the 896−910 antibody. Lane D, enzyme trypsinized in RbCl; lane E, enzyme trypsinized in NaCl. Positions of molecular weight markers (kDa) are indicated.

of clustering of the IMPs (Figure 3A) and were—after decoding—found to belong to the control samples. The remaining samples showed variable degrees of IMP clustering (Figure 3C,F), but with the most pronounced clustering for the samples trypsinized in Na^+ (Figure 3F). The overall frequency of IMPs was approximately the same under all conditions, consistent with our previous studies of trypsinized shark membranes (*32*).

The control membranes showed large (about 10 nm) intramembrane particles on the P-face (i.e., the cytoplasmic leaflet) of the cell membrane, after freeze-fracture. The IMPs were distributed mainly as single particles, but some formed small clusters (Figure 3A). Only occasional particles were present on the E-face (i.e., the extracellular leaflet) of the cell membrane. Under negative staining, control membranes showed a uniform distribution of distinct surface particles with a diameter of about 5 nm with only a small tendency for alignment in rows or clustering (Figure 3B).

Membranes, treated with trypsin in the presence of Rb^+ and freeze-fractured, appeared similar to control membranes, except that the IMPs were slightly more clustered (Figure 3C). By negative staining, some membranes exhibited small surface particles similar to those of controls, but they were less distinct and more clustered (Figure 3D). However, the majority of surfaces of the Rb-trypsinized membranes showed no distinct particles by negative staining (Figure 3E).

Membranes, treated with trypsin in the presence of Na^+ and freeze-fractured, showed IMPs that were more clustered than in controls or in most membranes treated with trypsin in the presence of Rb^+ (Figure 3F). Negative staining showed no distinct surface particles on membranes trypsinized in Na^+. The majority of membranes showed completely smooth surfaces (Figure 3H), but on some membrane surfaces, there were irregular areas that exhibited a slightly granular surface and were separated by smooth regions (Figure 3G).

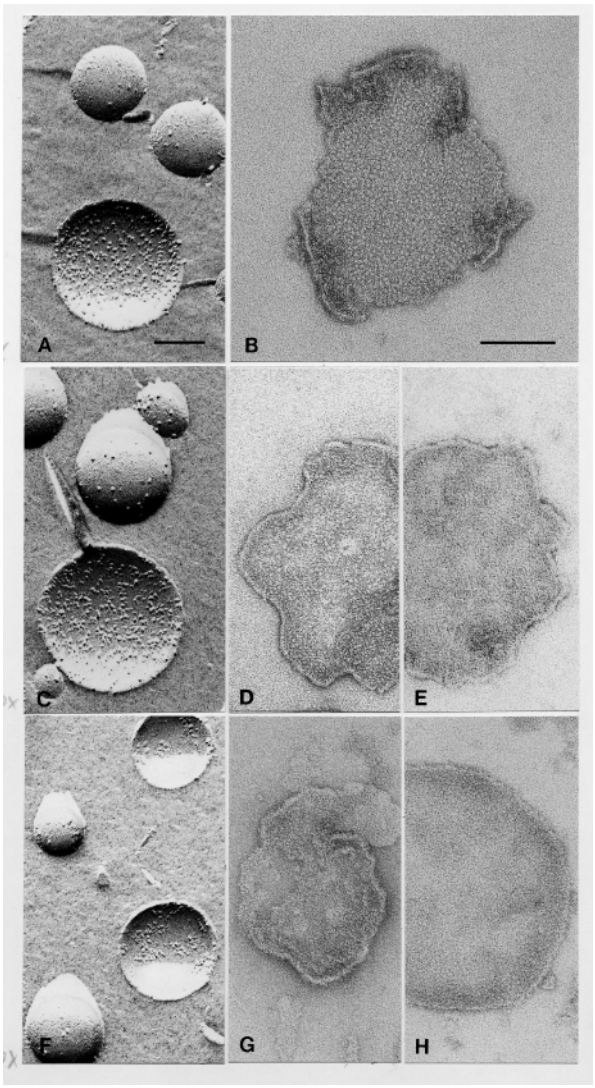

FIGURE 3: Electron micrographs of control and trypsinized preparations. Shark Na,K-ATPase membranes incubated with Rb^+ in the absence of trypsin (control enzyme, panels A and B), with trypsin in the presence of Rb^+ (panels C−E), and with trypsin in the presence of Na^+ (panels F−H). The membranes were either freeze-fractured (panels A, C, and F) or negatively stained with uranyl acetate (panels B, D, E, G, and H). The bars represent 0.1 μm, with the scale being the same within the group of freeze-fractured images (panels A, C, and F) and within the group of negatively stained images (panels B, D, E, G, and H).

Peptide Composition of Trypsinized Membranes. The peptide content of the trypsinized membranes separated by gel electrophoresis was characterized by N-terminal sequence analysis and by epitope mapping, using sequence-specific antibodies, see Table 1 and Figure 2. In separate Western experiments, all the antibodies were shown to react with the nontrypsinized (native) α-subunit and were thus expected to react with the same epitopes, if present, in the trypsinized membranes.

Rb^+-trypsinized membranes contain all the membrane-spanning fragments in addition to the β-subunit, as found previously (*18*). This is confirmed here by epitope-identification using antibodies, see Table 1. For the M5/M6 fragment, the 822−835 epitope at the C-terminal portion is recognized, and this, together with identification of the N-terminal sequence starting at Q^{744}, demonstrates that this fragment contains both M5 and M6, in agreement with the apparent

Table 1: Characterization of Rb- and Na-Trypsinized Preparations by Sequence and Epitope Analysis

Sequence Analysis

mass[a] (kDa)	fragment	shark sequence	Rb-trypsinized[a]	Na-trypsinized
11.5	M1/M2[b]	[75]DGPNSLTPPP	DGPNx[c] LTPPP	xPGNxLTPP
8.0	M3/M4[d]	[270]IATLASGL	IATLASGL	IATLAxGL
7.8	M5/M6[e]	[744]QAADMILL	QAxDxILL	not found[f]
19	M7-M10[g]	[841]TDKLVNERL	xDKLVNERL	not found[f]

Epitope Recognition

	Rb-trypsinized membranes			Na-trypsinized membranes		
antibody[h]	reaction	mass (kDa)	fragment	reaction	mass (kDa)	fragment
822−835	positive	7.8	M5/M6	negative[i]		
896−910	positive	19	M7-M10	positive	9.1	L7/L8
1009−1023	positive	19	M7-M10	negative[i]		

[a] Data from ref *18*. [b] N-Terminal residue of M1 is 36 in SERCA and 68 in pig kidney. [c] x denotes ambiguity in assignment from the amino acid sequence analysis. [d] N-Terminal residue of M3 is 235 in SERCA and 263 in pig kidney. [e] N-Terminal residue of M5 is 731 in SERCA and 737 in pig kidney. [f] Not found indicates that none of the sequences obtained from the gels were identical to parts of the shark sequence. [g] N-Terminal of M7 is 826 in SERCA and 834 in pig kidney. [h] Cf. ref *24*. [i] Negative indicates that the Western blots of the gels did not show recognition of this antibody.

molecular mass of 8 kDa. Epitopes with residues 896−910 (Figure 2, lane E) and with the C-terminus (1009−1023, Western blot not shown) are identified in the 19-kDa fragment of Rb^+-trypsinized membranes, as expected from the molecular mass of this fragment.

The Na^+-trypsinized membranes have not been previously characterized structurally. The fragments corresponding to M1/M2 and M3/M4 are identified here from N-terminal sequences of tryptic fragments with the same size as found for Rb^+-trypsinized membranes, suggesting that the cleavage sites in this part of the protein are identical for Rb^+- and Na^+-trypsinized membranes. However, N-terminal sequences of M5/M6 or of M7-M10 could not be identified in the gels. Numerous minor bands staining with Coomassie Blue were sequenced, but none of the bands were found to belong to the shark α-subunit sequence. Most sequences were apparently mixtures of several peptides, prohibiting clear identification from N-terminal sequencing. In contrast, by using the antibody technique, we could identify the 896−910 epitope of the extracellular L7/L8 loop in a 9.1-kDa fragment from the Na^+-trypsinized membranes (Figure 2, lane E). This shows that the L7/L8 loop is associated with the membranes, which—in view of the apparent molecular mass of about 9.1 kDa—demonstrates that M8 is present in the preparation, and the size of the fragment suggests that either M7 or M9 is also present in the preparation forming a hairpin with M8 (see Discussion).

Neither the 822−835 epitope, which is in the C-terminal part of M6, nor the C-terminal 1009−1023 epitope of M10 could be identified in the Na^+-trypsinized membranes on gels. This suggests that M6 is absent (and probably also M5, because there are no trypsin-sensitive bonds in the L5/L6 loop connecting M5 and M6) and also that the C-terminal end of the α-sububit is cleaved, possibly at the arginines around positions 1010−1016. In contrast to the Rb^+-trypsinized preparation, the membrane-spanning peptides M5, M6, M7, M9, and M10 are not directly identifiable in the Na^+-trypsinized preparation (but either M7 or M9 is probably present together with M8).

ESR-Spectroscopy of Trypsinized Membranes. The effects of either glycerol or PEG in the suspending medium on the rotational mobility of the spin-labeled Na,K-ATPase in native and trypsinized membranes were studied by using saturation transfer ESR spectroscopy. Conventional ESR spectra of the 5-MeClHgMSL spin label attached to the Na,K-ATPase evidence little or no segmental motion of the label relative to the protein and contain only a very small proportion of a highly mobile spin label component, see Figure 4A. This spin label is therefore suitable for determining rotational motion of the entire protein assembly.

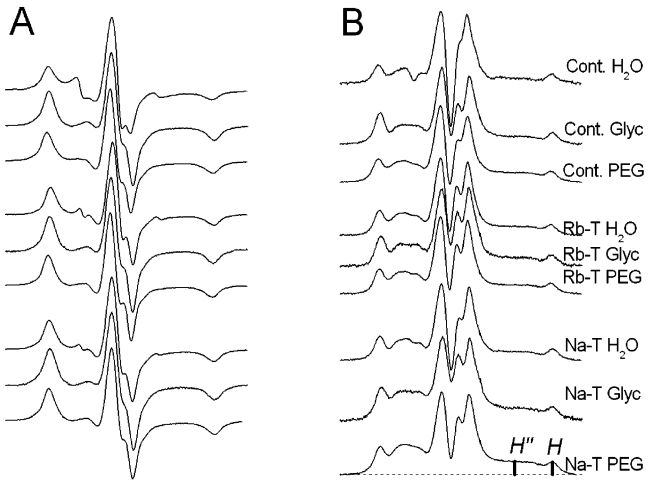

FIGURE 4: ESR spectra at 4 °C of chloromercuri-spin-labeled (5-MeClHgMSL) Na,K-ATPase. (A) Three sets of conventional ESR spectra. The upper set contains control enzyme (Cont.), and the membranes are suspended in buffer alone or in the presence of either 75% glycerol (Glyc) or 50% poly(ethylene glycol) (PEG). The middle and lower sets are of membranes in which the enzyme was trypsinized in the presence of RbCl (Rb-T) or NaCl (Na-T), respectively, and suspended in the same three media. (B) The corresponding second harmonic, 90° out-of-phase absorption STESR spectra (V_2'-display). In the bottom spectrum in panel B, the spectral positions at which the STESR diagnostic line heights H'' and H are measured are indicated. Total scan width = 10 mT.

Figure 4B shows STESR spectra (V_2'-display) of Na,K-ATPase membranes labeled with 5-MeClHgMSL that are suspended in buffer or in aqueous solutions of 75% glycerol or 50% PEG, at 4 °C. For control enzyme (top three spectra), the line heights in the diagnostic regions of the spectra at low and high field increase, as expected for decreasing rotational mobility of the spin-labeled protein, with 50% PEG in the suspending medium (*33*, *34*). Changes qualitatively

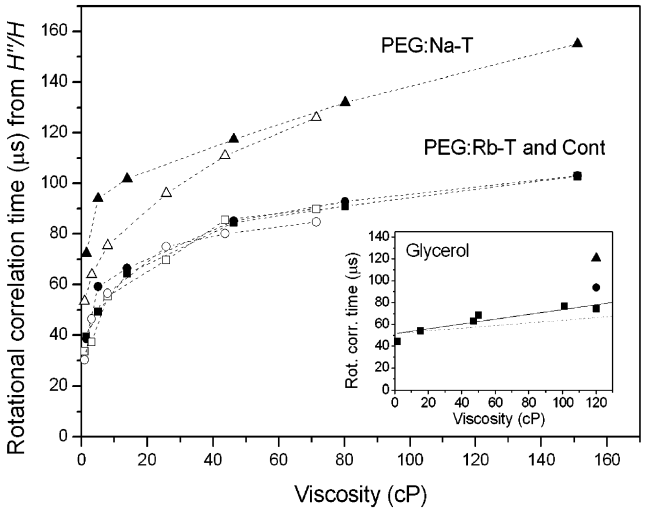

FIGURE 5: Dependence on viscosity of the suspending medium of the rotational correlation time, τ_R^{eff}, deduced from the H''/H line-height ratio in the STESR spectra of Na,K-ATPase preparations labeled with 5-MeClHgMSL. Data are shown for control enzyme (squares) and for enzyme trypsinized in the presence of RbCl (circles) or in the presence of NaCl (triangles), suspended in PEG-solutions. The filled symbols are for STESR spectra obtained at 4 °C, and the open symbols are for STESR spectra obtained at 20 °C. In the inset, data obtained at 4 °C are shown for control enzyme (squares), for Rb-T (circle), and for Na-T (triangle); the latter two are shown only in 75% glycerol. The solid straight line has an intercept of 52 μs and a slope of 22 μs/P, and the dotted straight line has the same intercept with a slope of 12 μs/P.

similar to those with PEG, but to a smaller extent, are observed in the STESR spectra of the spin-labeled protein from membranes suspended in a 75% glycerol solution (Figure 4B, top). For the Rb-trypsinized preparations (Figure 4B, middle), the spectra are qualitatively similar to those of the control enzyme, apart from the absence of the mobile component in the spectrum from the sample in buffer. STESR spectra of the Na-trypsinized preparation indicate decreased rotational mobility compared to control enzyme, both in buffer alone and in the presence of glycerol or PEG (Figure 4B, bottom).

Figure 5 compares the rotational correlation times deduced from the high-field diagnostic STESR line height ratios (H''/H, spectral positions are shown in the bottom spectrum in Figure 4B) for the three preparations containing PEG (at 4 °C, filled symbols, and at 20 °C, open symbols) or glycerol (at 4 °C, see inset to Figure 5). Control enzyme in the presence of glycerol (filled squares in inset) responds to the increase in viscosity as expected for a particle experiencing an increased hydrodynamic drag. The solid straight line in Figure 5 (inset) represents the predicted viscosity dependence if ca. 60% of the protein is external to the membrane (*34*). With PEG, the relation between rotational correlation time and viscosity does not conform to the simple linear relation found for glycerol. For control enzyme (squares), as well as for both trypsinized preparations, PEG appears to cause aggregation of the protein. This was observed earlier for control enzyme (*34*), and the trypsinized preparations appear to behave similarly. For the Rb-trypsinized preparation (circles), there is a strong similarity to control enzyme (compare squares and circles in Figure 5). For Na-trypsinized enzyme (triangles), the increase in rotational correlation time with viscosity is even stronger than for Rb-trypsinized enzyme.

Also included in Figure 5 (inset) are data from trypsinized preparations in 75% glycerol, at 4 °C. Glycerol leads to an increase in correlation time of the trypsinized samples, relative to that of control enzyme. This finding suggests that the structure of the trypsinized membranes differs from that of the control enzyme, to an extent beyond simple removal of parts of the protein. The data suggest either that there is a reorientation of the spin-label population in the trypsinized membranes relative to that of control enzyme or that the proteins remaining in the trypsinized preparations are aggregated compared to control enzyme (see later Discussion).

DISCUSSION

It was shown previously, by identification of amino-terminal sequences of peptide fragments, that the Rb-trypsinized preparation from shark contains the M1/M2, M3/M4, M5/M6, and M7-M10 transmembrane domains (*18*). Additionally, electron microscopy showed intramembranous particles in the Rb-trypsinized preparations that are of the same size and density as in native membranes (*32*).

Transmembrane Peptides in Na-Trypsinized Preparations. From N-terminal sequencing, we find that membranes with enzyme trypsinized in the presence of Na^+ contain peptide fragments corresponding to M1/M2 and M3/M4, and a fragment containing the L7/L8 loop is identified from labeling with an antibody to residues 896−910 (Table 1). In the Na-trypsinized preparation, it was not possible to identify amino acid sequences corresponding to other putative tryptic splits of the α-subunit. In addition, an antibody against the M5/M6 peptide, which clearly recognizes this peptide in Rb-trypsinized membranes, failed to detect the 822−835 epitope in the Na-trypsinized preparation. Similarly, the antibody to C-terminal residues 1009−1023 did not recognize peptides in the Na-trypsinized preparation, suggesting that the C-terminal part of the α-subunit is truncated. Taken together with the absence of a 19-kDa Coomassie Blue staining fragment in SDS gels, this demonstrates that extensive tryptic degradation in the presence of Na^+ is very different from that in the presence of K^+ (or Rb^+). It should be recalled that the water-soluble peptides are removed by repeated centrifugation of the membranes. For kidney Na,K-ATPase, it is well-known that the initial tryptic splits are sensitive to Na^+ and K^+ (*35*), but the difference between extensively trypsinized Na- and K-forms found here for shark Na,K-ATPase was not reported with the kidney Na,K-ATPase (*8*). We detect the L7/L8 loop associated with the membrane in shark Na-trypsinized preparations, and the mass of the peptide (about 9.1 kDa) is such that the loop can be in the middle of a hairpin consisting of transmembrane segments M7 and M8 or in the N-terminal part of a hairpin of segments M8 and M9. The failure to recognize the epitope containing residues 822−835 precludes the presence of a putative 9.1 kDa M6/M7-peptide with a C-terminal 896−910 epitope. Since there are several trypsinization sites in the regions flanking the M8 peptide, the structure of the peptide containing the L7/L8 epitope cannot be unequivocally deduced. In the subsequent modeling, we have assumed that a M7/M8 peptide includes residues 834−910 and that a M8/M9 peptide includes residues 895−977 (using the shark sequence).

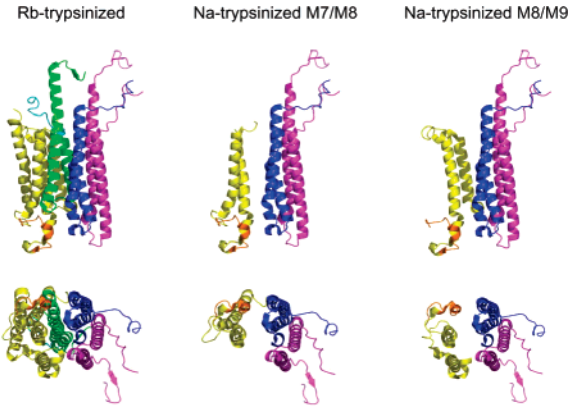

FIGURE 6: Disposition of protein in trypsinized membranes. Using the Ca-ATPase crystal structure (*5*), we show the peptides corresponding to the transmembrane segments (see Figure 1 for SERCA residue numbers). The color code is magenta (M1/M2), blue (M3/M4), green (M5/M6), and yellow (M7-M10). The cyan part of the M5/M6 peptide is the antibody 822−835 recognition site, and the orange part of M7-M10 is the 896−910 site (loop L7/L8). In the upper row, the side view (i.e., within the plane of the membrane) is shown for Rb-trypsinized membranes (left-hand column) and for Na-trypsinized membranes in two states: with M7/M8 (middle column, SERCA residues 827−917) or with M8/M9 present (right-hand column, SERCA residues 865−956). The lower row gives the corresponding views from the extracellular side. This figure was prepared using PyMOL (*49*).

Ultrastructure of Trypsinized Membranes. Freeze-fracture electron microscopy of membranes trypsinized in the presence of NaCl or RbCl suggests a similar number of intramembranous particles in the two preparations, but with a tendency to more extensive aggregation of the particles in Na-trypsinized membranes. Furthermore, we observe the presence of intramembranous particles of the same size in Na-trypsinized preparations as in the native or Rb-trypsinized preparations (Figure 3A,C,F). This suggests that, despite the more extensive degradation of the α-subunit in Na-trypsinized membranes than in Rb-trypsinized membranes, the remaining peptides (together with the *β*-subunit) still form clusters of about the same size as in the native enzyme. In Na- and Rb-trypsinized preparations, most membranes were devoid of surface particles when visualized by negative staining (Figure 3E,H). These surfaces may be cytoplasmic membrane surfaces, where the intracellular loops of the α-subunit have been digested. Some membranes in both preparations showed small and less distinct surface particles, which were often clustered (Figure 3D,G). These particles may represent *β*-subunits exposed on the external membrane face.

The structural consequences of trypsinization can be discussed by using the three-dimensional disposition of the Ca-ATPase as a model. In Figure 6, the overall crystal structure is dissected in such a manner that only the tryptic fragments are shown. For Rb-trypsinized enzyme, this dissection is relatively unambiguous because the N-terminal sequences and approximate sizes of the peptides are known. Figure 6 shows the side view of the helix bundle, as well as the top and bottom views perpendicular to the membrane. For Na-trypsinized enzyme, it is clear that M1/M2 and M3/M4 are present, but for the remaining peptides, there are several possibilities. Two alternative models with two transmembrane segments attached to the L7/L8 loop are shown, but M5/M6 is omitted. Clearly, the absence of the M5/M6 segment leaves both a M7/M8 and a M8/M9 peptide at some distance from the M1/M2/M3/M4 cluster. With the nonidentified peptides in Na-trypsinized enzyme dissociated from the membrane, it is evident that reorganization and possibly aggregation are much more likely for Na-trypsinized than for Rb-trypsinized enzyme, because the latter remains essentially native in the transmembrane region.

Effect of PEG on Rotational Motion. The effective rotational correlation times of the spin-labeled protein do not conform to a simple linear dependence on external viscosity, neither for control enzyme (*18*) nor for the trypsinized preparations (see Figure 5). Correlation times for suspensions in PEG are all larger than for those in glycerol at the same viscosity, indicating a PEG-induced aggregation both of the native protein and of the trypsinized membranes. The remarkable similarity between the control enzyme and the Rb-trypsinized preparation indicates that the major restraints on rotational motion of the two may be similar, also with respect to PEG-induced aggregation. PEG-induced aggregation is observed both at 4 °C and at 20 °C and appears to be similar at the two temperatures for control and Rb-trypsinized membranes, whereas the effect of PEG is more marked at the lower temperature for Na-trypsinized membranes.

PEG will, in addition to changing viscosity, also effectively reduce the water activity. Because the largest portion of extramembranous α-subunit is cleaved and removed by trypsin in the presence of Na^+, it might be expected that the effect of decreasing water activity on hydration forces is lowest for this preparation, followed next by the Rb-trypsinized form, with the maximum effect being expected for the native protein (*34*). However, in the presence of increasing aqueous concentrations of PEG, the rotational correlation time is maximal with the Na-trypsinized form, for which it is considerably larger than for Rb-trypsinized or native membranes. Evidently, the controlling factor in Na-trypsinized membranes is the absolute reduction in hydration repulsion between proteins by removal of the hydrated (extramembrane) portions of the enzyme. This then increases the propensity to aggregation and hence also the susceptibility to PEG.

Effect of Glycerol on Rotational Diffusion. In Figure 5 (inset), the rotational correlation time for control enzyme is fitted as a function of the aqueous viscosity with increasing glycerol by a line with intercept ($\tau_R^{eff} = 52$ *μ*s) and a slope of 22 *μ*s/P. The ratio between these two parameters is a measure of the ratio between the extramembranous and the total volumes of the protein (*34*). If the effective viscosity of the membrane is taken to be 5 P (*36*), the extramembranous volume is calculated to be 69% of the total, that is, 108 kDa. This gives a membrane-embedded molecular mass of about 50 kDa, which is larger than expected for the transmembrane segments alone (about 26 kDa, see ref *30*). Possible explanations for this discrepancy are that the viscosity of the membrane is larger or that more protein is imbedded in the membrane than the putative transmembrane stretches alone.

Trypsin releases an extramembranous mass of about 63 kDa of the total volume of an α*β*-protomer (see Materials and Methods). The mass of the protein and carbohydrate external to the membrane should decrease from about 132

kDa (158 kDa total mass, minus 26 kDa intramembranous protein) to about 69 kDa in the trypsinized $\alpha\beta$-protomer. The relation between the rotational correlation time and the extramembranous viscosity predicted under these circumstances is shown by the dotted line in Figure 5 (inset), which has a slope of 12 μs/P. In the absence of glycerol, there is no appreciable effect of trypsinization in Rb^+, but at 75% glycerol, the rotational motion is restricted in the trypsinized preparation relative to the control, that is, an effect opposite the one expected from removal of aqueous domains of the protein. The data for the trypsinized preparations clearly do not follow a simple model where 39% of extramembranous volume is released by trypsin (see Materials and Methods).

This lower average rotational mobility for the Rb-trypsinized complexes in glycerol can perhaps be explained by considering either that a fraction of the peptide fragments is involved in forming larger aggregates or that the shape of the tryptic complex is very different from the cylindrical shape tacitly assumed for the nontrypsinized enzyme. If the native $(\alpha\beta)_2$-diprotomer has an axial ratio of about 2.5 (*37*), this ratio for the internal side of the trypsinized protein would have to increase to about 10 if the rotational correlation time is to remain unchanged after Rb-trypsinization (see, e.g., ref *18*). An additional consideration is that the β-subunit carries the major mass of the protein (and all the carbohydrate) on the external side of the membrane, about 37 kDa, whereas the minor stretches of external α-subunit have a mass of only about 8 kDa. It is therefore possible that the glycosylated β-subunit, which is not cleaved by trypsin, may make a disproportionately large contribution to the effects of aqueous drag on the rotating protein assembly. A further possibility is that the spin-label orientation changes on trypsinization in such a way as to compensate for changes in effective STESR correlation time with size of the rotating species (*38*, *39*). This would require that trypsinization leaves the spin-label principal axis oriented closer to the rotation axis, on average, than in control enzyme, either by internal rearrangement or by removal of part of the covalent spin-label population.

Our present, and previous (*18*), results with Na-trypsinized membranes indicate that the tryptic peptides undergo aggregation to form a complex of larger molecular mass in the membrane. This complex therefore is expected also to have a larger volume of the exposed tryptic ends, which collectively are responsible for the effect of aqueous viscosity relative to that in Rb-trypsinized preparations.

Structural and Functional Aspects of Aggregation and the M5/M6 Hairpin. Aggregation of the peptides remaining after trypsinization in Na^+ is possible for a number of reasons. Removal of M10 and M9 (or M10 and M7) will leave parts of the remaining peptides more exposed to the hydrophobic lipid bilayer (Figure 6, lower panel). To reduce contact with the lipids, the M7/M8 (or M8/M9) peptide must reorient itself toward either the M1-M4 bundle of helices or the neighboring peptide clusters (cf. Figure 3F−H), the latter leading to aggregation. The requirement for reorganization is also underlined by the absence of the M5/M6 segment (cf. Figure 6, lower panel), which leaves a void in the middle of the peptide cluster. Therefore, reorganization of the structure must occur, and possibly aggregation.

The loss of the M5/M6 tryptic hairpin has been observed for Na,K-ATPase under several conditions. Lutsenko et al. (*40*) demonstrated that incubation of trypsinized kidney enzyme at 37 °C for a few minutes led to dissociation of M5/M6 from the membrane. Possibly, the shark membranes express this lability already at room temperature, where our trypsinization is carried out. Shainskaya et al. (*41*) showed that trypsinization first leads to loss of Rb-occlusion ability, and subsequently, M5/M6 is released from the membranes.

Sweadner and co-workers (*42*, *43*) have shown that the β-subunit interacts with M7, in a study where M8, M9, and M10 are shown to dissociate from kidney membranes upon heat treatment and subsequently become accessible to proteolytic enzymes. This could also suggest that we have M7 present and thus that the M7/M8-hairpin is the one remaining after trypsinolysis of shark membranes. The L7/L8-loop is also known to interact strongly with the β-subunit, which perhaps explains why it is retained in the Na-trypsinized membranes (*44*), that is, a steric protection by the extracellular parts of the β-subunit. Proteolysis sites between M8 and M9, as well as after M10 but before the C-terminal site, were also demonstrated (*43*). This is in line with our observations, especially that the C-terminal antibody does not react with our Na-trypsinized preparation and that M9/M10 leaves the membrane as a result of heat denaturation at 50−55 °C (*43*). This is similar to our findings on membranes trypsinized in Na^+ but simply occurring at a lower temperature for shark.

Goldshleger et al. (*45*) also show that, depending on the conditions for heat treatment, the α-subunit is cleaved between M8 and M9 and between M9 and M10. They conclude that M8 and M9 leave the membrane after thermal denaturation. For cytoplasmic trypsinolysis, they find a 10-kDa fragment containing M7 and M8, as found for the Na-trypsinized shark enzyme. A similar 10-kDa peptide was obtained from digestion of the H,K-ATPase (*46*, *47*). Proteinase K treatment of Ca-ATPase yields a C-terminal 19-kDa fragment similar to that obtained for Na,K-ATPase, but the ability to bind Ca^{2+} with high affinity is lost (*25*). The difference between these two P-type enzymes could lie in a stabilizing effect of the β-subunit.

Conclusion. In conclusion, we have shown that the structural integrity of the M1−M4 helix cluster is retained, even with a degraded 19-kDa fragment and probable loss of M5/M6 in Na-trypsinized membranes. The β-subunit could play a stabilizing role here. The lack of Rb-occlusion capacity in Na-trypsinized preparations (*18*) is consistent with removal of the M5/M6 segment, which is thought from mutagenesis studies to contribute to the occlusion cage (see e.g., ref *48*). The aggregating effects of PEG are also found with both trypsinized preparations, suggesting that the aggregation could, nonetheless, be potentiated by reducing the hydrated surface of the protein.

ACKNOWLEDGMENT

The authors thank Birthe Bjerring Jensen, Angielina Damgaard, and Karen Thomsen for excellent technical assistance. The spin label 5-MeClHgMSL was a kind gift from Dr. Kalman Hideg, and the antibodies were a kind gift from Dr. Jesper V. Møller.

REFERENCES

1. Møller, J. V., Juul, B., and le Maire, M. (1996) Structural organization, ion transport, and energy transduction of P-type ATPases, *Biochim. Biophys. Acta 1286*, 1−51.

2. Kaplan, J. H. (2002) Biochemistry of Na,K-ATPase, *Annu. Rev. Biochem. 71*, 511−535.
3. Hebert, H., Purhonen, P., Vorum, H., Thomsen, K., and Maunsbach, A. B. (2001) Three-dimensional structure of renal Na,K-ATPase from cryo-electron microscopy of two-dimensional crystals, *J. Mol. Biol. 314*, 479−494.
4. Rice, W. J., Young, H. S., Martin, D. W., Sachs, J. R., and Stokes, D. L. (2001) Structure of Na^+,K^+-ATPase at 11-Å resolution: comparison with Ca^{2+}-ATPase in E1 and E2 states, *Biophys. J. 80*, 2187−2197.
5. Toyoshima, C., Nakasako, M., Nomura, H., and Ogawa, H. (2000) Crystal structure of the calcium pump of sarcoplasmic reticulum at 2.6 Å resolution, *Nature 405*, 647−655.
6. Toyoshima, C., and Nomura, H. (2002) Structural changes in the calcium pump accompanying the dissociation of calcium, *Nature 418*, 605−611.
7. Sørensen, T. L.-M., Møller, J. V., and Nissen, P. (2004) Phosphoryl transfer and calcium ion occlusion in the calcium pump, *Science 304*, 1672−1675.
8. Karlish, S. J. D., Goldschleger, R., and Stein, W. D. (1990) A 19-kDa C-terminal tryptic fragment of the α-chain of Na/K-ATPase is essential for occlusion and transport of cations, *Proc. Natl. Acad. Sci. U.S.A. 87*, 4566−4570.
9. Or, E., Goldshleger, R., Shainskaya, A., and Karlish, S. J. D. (1998) Specific cross-links between fragments of proteolyzed Na,K-ATPase induced by *o*-phthalaldehyde, *Biochemistry 37*, 8197−8207.
10. Or, E., Goldshleger, R., and Karlish, S. J. D. (1999) Characterization of disulfide cross-links between fragments of proteolyzed Na,K-ATPase. Implications for spatial organization of transmembrane helices, *J. Biol. Chem. 274*, 2802−2809.
11. Or, E., Goldshleger, R., Tal, D. M., and Karlish, S. J. D. (1996) Solubilization of a complex of tryptic fragments of Na,K-ATPase containing occluded Rb ions and bound ouabain, *Biochemistry 35*, 6853−6864.
12. Sarvazyan, N. A., Ivanov, A., Modyanov, N. M., and Askari, A. (1997) Ligand-sensitive interactions among the transmembrane helices of Na^+/K^+-ATPase, *J. Biol. Chem. 272*, 7855−7858.
13. Liu, L., and Askari, A. (1997) Evidence for the existence of two ATP-sensitive Rb+ occlusion pockets within the transmembrane domains of Na^+/K^+-ATPase, *J. Biol. Chem. 272*, 14380−14386.
14. Corbalan-Garcia, S., Teruel, J., Villalain, J., and Gomez-Fernandez, J. (1994) Extensive proteolytic digestion of the (Ca^{2+}+Mg^{2+})-ATPase from sarcoplasmic reticulum leads to a highly hydrophobic proteinaceous residue with a mainly α-helical structure, *Biochemistry 33*, 8247−8254.
15. Raussens, V., le Maire, M., Ruysschaert, J.-M., and Goormaghtigh, E. (1998) Secondary structure of the membrane-bound domains of H^+,K^+-ATPase and Ca^{2+}-ATPase, a comparison by FTIR after proteolysis treatment of the native membranes, *FEBS Lett. 437*, 187−192.
16. Raussens, V., De Jongh, H., Pézolet, M., Ruysschaert, J.-M., and Goormaghtigh, E. (1998) Secondary structure of the intact H^+,K^+-ATPase and of its membrane-embedded region. An attenuated total reflection infrared spectroscopy, circular dichroism and Raman spectroscopy study, *Eur. J. Biochem. 252*, 261−267.
17. Heimburg, T., Esmann, M., and Marsh, D. (1997) Characterization of the secondary structure and assembly of the transmembrane domains of trypsinized Na,K-ATPase by Fourier transform infrared spectroscopy, *J. Biol. Chem. 272*, 25685−25692.
18. Esmann, M., Karlish, S. J. D., Sottrup-Jensen, L., and Marsh, D. (1994) Structural integrity of the membrane domains in extensively trypsinized Na,K-ATPase from shark rectal glands, *Biochemistry 33*, 8044−8050.
19. Esmann, M., Sar, P. C., Hideg, K., and Marsh, D. (1993) Maleimide-, iodoacetamide-, indanedione- and chloromercuric-spin label reagents with derivatized nitroxide rings as ESR reporter groups for protein conformation and dynamics, *Anal. Biochem. 213*, 336−348.
20. Skou, J. C., and Esmann, M. (1979) Preparation of membrane bound and of solubilized Na,K-ATPase from rectal glands of *Squalus acanthias*, *Biochim. Biophys. Acta 567*, 436−444.
21. Esmann, M. (1988) ATPase and phosphatase activity of the Na,K-ATPase; molar and specific activity, protein determinations, *Methods Enzymol. 156*, 105−115.
22. Schagger, H., and von Jagow, G. (1987) Tricine-sodium dodecyl sulfate-polyacrylamide gel electrophoresis for the separation of proteins in the range from 1 to 100 kDa, *Anal. Biochem. 166*, 369−379.
23. Matsudaira, P. (1987) Sequence from picomole quantities of proteins electroblotted onto polyvinylidene difluoride membranes, *J. Biol. Chem. 262*, 10035−10038.
24. Ning, G., Maunsbach, A. B., Lee, Y.-J., and Møller, J. V. (1993) Topology of Na,K-ATPase α subunit epitopes analyzed with oligopeptide-specific antibodies and double-labeling immunoelectron microscopy, *FEBS Lett. 336*, 521−524.
25. Juul, B., Turc, H., Durand, M. L. Gomez de Gracia, A., Denoroy, L., Møller, J. V., Champeil, M., and le Maire, M. (1995) Do transmembrane segments in proteolyzed sarcoplasmic reticulum Ca^{2+}-ATPase retain their functional Ca^{2+} binding properties after removal of cytoplasmic fragments by proteinase K? *J. Biol. Chem. 270*, 20123−20134.
26. Fajer, P., and Marsh, D. (1982) Microwave and modulation field inhomogeneities and the effect of cavity Q in saturation transfer ESR spectra. Dependence on sample size, *J. Magn. Reson. 49*, 212−224.
27. Esmann, M., Horváth, L. I., and Marsh, D. (1987) Saturation-transfer electron spin resonance studies on the mobility of spin-labeled sodium and potassium ion activated adenosinetriphosphatase in membranes from *Squalus acanthias*, *Biochemistry 26*, 8675−8683.
28. Hemminga, M. A., De Jaeger, P. A., Marsh, D., and Fajer, P. (1984) Standard conditions for the measurement of saturation-transfer ESR spectra, *J. Magn. Reson. 59*, 160−163.
29. Marsh, D. (1998) Spin label ESR spectroscopy and FTIR spectroscopy for structural/dynamic measurements on ion channels, *Methods Enzymol. 294*, 59−92.
30. Karlish, S. J. D. (1997) Organization of the membrane domain of the Na/K-pump, *Ann. N. Y. Acad. Sci. 834*, 30−44.
31. Esmann, M., Christiansen, C., Karlsson, K.-A., Hansson, G. C., and Skou, J. C. (1980) Hydrodynamic properties of solubilized Na,K-ATPase from rectal glands of *Squalus acanthias*, *Biochim. Biophys. Acta 603*, 1−12.
32. Ning, G., Esmann, M., and Maunsbach, A. B. (1993) Ultrastructure of membrane-bound Na,K-ATPase after extensive tryptic digestion, *FEBS Lett. 330*, 19−22.
33. Thomas, D. D., Dalton, L. R., and Hyde, J. S. (1976) Rotational diffusion studied by passage saturation transfer electron paramagnetic resonance, *J. Chem. Phys. 65*, 3006−3024.
34. Esmann, M., Hideg, K., and Marsh, D. (1994) Influence of poly(ethylene glycol) and aqueous viscosity effects on the rotational diffusion of Na,K-ATPase, *Biochemistry 33*, 3693−3697.
35. Jørgensen, P. L. (1975) Purification and characterization of Na,K-ATPase. V. Conformational changes in the enzyme. Transitions between the Na-form and the K-form studied with tryptic digestion as a tool, *Biochim. Biophys. Acta 401*, 399−415.
36. Cherry, R. J., and Godfrey, R. E. (1981) Anisotropic rotation of bacteriorhodopsin in lipid membranes. Comparison of theory with experiment, *Biophys. J. 36*, 257−276.
37. Hebert, H., Skriver, E., and Maunsbach, A. B. (1985) Three-dimensional structure of renal Na,K-ATPase determined by electron microscopy of membrane crystals, *FEBS Lett. 187*, 182−186.
38. Robinson, B. H., and Dalton. L. R. (1980) Anisotropic rotational diffusion studied by passage saturation transfer EPR, *J. Chem. Phys. 72*, 1312−1324.
39. Marsh, D., and Horváth, L. I. (1989) Spin-label studies of the structure and dynamics of lipids and proteins in membranes, in *Advanced EPR. Applications in Biology and Biochemistry* (Hoff, A. J., Ed.) pp 707−752, Elsevier, Amsterdam.
40. Lutsenko, S., Anderko, R., and Kaplan, J. H. (1995) Membrane disposition of the M5-M6 hairpin of Na^+,K^+-ATPase α subunit is ligand dependent, *Proc. Natl. Acad. Sci. U.S.A. 92*, 7936−7940.
41. Shainskaya, A., Nesaty, V., and Karlish, S. J. D. (1995) Interactions between fragments of trypsinized Na,K-ATPase detected by thermal inactivation of Rb^+ occlusion and dissociation of the M5/M6 fragment, *J. Biol. Chem. 273*, 7311−7319.
42. Donnet, C., Arystarkhova, E., and Sweadner, K. J. (2001) Thermal denaturation of the Na,K-ATPase provides evidence for α-α oligomeric interaction and γ subunit association with the C-terminal domain, *J. Biol. Chem. 276*, 7357−7365.
43. Arystarkhova, E., Gibbons, D. L., and Sweadner, K. J. (1995) Topology of the Na,K-ATPase, *J. Biol. Chem. 270*, 8785−8796.

44. Colonna, T. E., Huynh, L., and Fambrough, D. M. (1997) Subunit interactions in the Na,K-ATPase explored with the yeast two-hybrid system, *J. Biol. Chem. 272*, 12366−12372.

45. Goldshleger, R., Tal, D. M., and Karlish, S. J. D. (1995) Topology of the α-subunit of Na,K-ATPase based on proteolysis. Lability of the topological organization, *Biochemistry 34*, 8668−8679.

46. Besancon, M., Shin, J. M., Mercier, M., Munson, K., Miller, M., Hersey, S., and Sachs, G. (1993) Membrane topology and omeprazole labeling of the gastric hydrogen ion-potassium-adenosinetriphosphatase, *Biochemistry 32*, 2345−2355.

47. Shin, J. M., and Sachs, G. (1994) Identification of a region of the H,K-ATPase alpha subunit associated with the beta subunit, *J. Biol. Chem. 269*, 8642−8646.

48. Jørgensen, P. L., and Petersen, P. A. (2001) Structure−function relationships of Na^+, K^+, ATP, or Mg^{2+} binding and energy transduction in Na,K-ATPase, *Biochim. Biophys. Acta 1505*, 57−74.

49. DeLano, W. L. (2002) The PyMOL Molecular Graphics System on World Wide Web, http://www.pymol.org

BI051573X